Phospholipid Scramblase 3 Controls Mitochondrial Structure, Function, and Apoptotic Response

Jihua Liu,[1] Qiang Dai,[1] Jun Chen,[1] David Durrant,[1] Angela Freeman,[1] Tong Liu,[1] Douglas Grossman,[1,3,4] and Ray M. Lee[1,2,4]

[1]Huntsman Cancer Institute, [2]Departments of Internal Medicine, [3]Dermatology, and [4]Oncological Sciences, University of Utah, Salt Lake City, UT

Abstract

Phospholipid scramblase 3 (PLS3) is a newly recognized member of a family of proteins responsible for phospholipid translocation between two lipid compartments. To study PLS3 function in mitochondria, we disrupted its conserved calcium-binding motif yielding an inactive mutant PLS3(F258V). Cells transfected with PLS3(F258V) exhibited reduced proliferative capacity. Mitochondrial analysis revealed that PLS3(F258V)-expressing cells have decreased mitochondrial mass shown by lower cytochrome *c* and cardiolipin (CL) content, poor mitochondrial respiration, and reduced oxygen consumption and intracellular ATP; whereas wild-type PLS3-transfected cells exhibit increased mitochondrial mass and enhanced respiration. Electron microscopic examination revealed that the mitochondria in PLS3(F258V)-expressing cells have densely packed cristae and are fewer in number and larger than those in control cells. The abnormal mitochondrial metabolism and structure in PLS3(F258V)-expressing cells were associated with decreased sensitivity to UV- and tBid-induced apoptosis and diminished translocation of CL to the mitochondrial outer membrane. In contrast, wild-type PLS3-transfected cells displayed increased sensitivity to apoptosis and enhanced CL translocation. These studies identify PLS3 as a critical regulator of mitochondrial structure and respiration, and CL transport in apoptosis.

Introduction

Regulation of apoptosis, or programmed cell death, is critical for development and tissue homeostasis, and dysregulation of apoptosis is a key factor in neoplastic transformation (1, 2). Apoptotic cell death is characterized by a proteolytic caspase cascade that emanates from either an 'extrinsic' pathway, initiated by membrane-bound death receptors leading to activation of caspase-8, or an 'intrinsic' pathway triggered by DNA-damaging drugs and UV radiation leading to mitochondrial depolarization and subsequent activation of caspase-9 (3).

Caspase activation leads to distinct morphological changes, including mitochondrial disintegration, followed by nuclear fragmentation, chromatin condensation, and cytoplasmic membrane blebbing (4, 5). An additional early morphological event in cells undergoing apoptosis is translocation of phosphatidylserine (PS) from the inner to the outer leaflet of the plasma membrane (6–8). Externalized PS is recognized by macrophages, which rapidly remove apoptotic cells by phagocytosis (9, 10).

Mitochondria are central integrators of most apoptotic pathways (11). Activation of the intrinsic pathway causes mitochondrial release of a number of pro-apoptotic molecules including cytochrome *c*, endonuclease G (12, 13), SMAC/Diablo (14, 15), and apoptosis-inducing factor (16). In addition, multiple pro-apoptotic regulators including Bax, Bad, Bid, Bim, p53, JNK, PKC-δ, nuclear receptor TR3 (11, 17), and the Peutz-Jegher gene product LKB1 (18) are translocated to mitochondria during apoptosis. In some cell types, the extrinsic pathway is linked to the intrinsic pathway via activation of caspase-8, which causes NH_2-terminal cleavage of Bid to generate tBid (19). The active tBid fragment is N-myristoylated (20) and then localizes to mitochondria through a positive interaction with cardiolipin (CL; 21). Activated tBid induces CL-dependent activation of Bax and Bak to form cytochrome *c* channels during apoptosis (22). In the absence of Bax and Bak, tBid is unable to induce cytochrome *c* release (23–25).

Phospholipid scramblases (PLS) are enzymes responsible for bidirectional movement of phospholipids (26), and four PLS family members have been identified (27). PLS1 is located in the plasma membrane and is responsible for translocation of phospholipids between the inner and outer leaflets (28). Although apoptotic PS translocation was unaltered in PLS1-deficient mice (29), the role of PLS1 in apoptosis remains unclear given the presence of additional enzymes associated with plasma membrane phospholipid translocation such as aminophospholipid translocase (26, 30, 31). PLS family members contain a conserved calcium-binding motif, and Zhou *et al.* (32) found that mutation of residues in this region of PLS1 completely eliminated enzymatic activity. PLS1 is phosphorylated at Thr-161 by PKC-δ, which translocates to the plasma membrane during apoptosis (33); in addition, PLS1 is phosphorylated at Tyr-69/74 by c-abl kinase (34). The role of calcium binding and these various phosphorylation events in PLS1 activation and regulation, however, remain to be determined.

A newly identified member of the scramblase family, designated PLS3, is localized to the mitochondria rather than plasma membrane (35). However, little is known regarding the

physiological function of PLS3 in mitochondria. We have shown previously that PLS3, like PLS1, is phosphorylated by PKC-δ (35). A mitochondrial targeted PKC-δ dramatically enhanced susceptibility to apoptosis in cells overexpressing PLS3, suggesting that PLS3 is the direct mitochondrial effector of PKC-δ-induced apoptosis (35). In this study, we report that the activity of PLS3 affects both mitochondrial structure and function, and modulates apoptotic translocation of CL from the mitochondrial inner membrane (IM) to the outer membrane (OM) and tBid-induced cytochrome *c* release.

Results

Both Wild-Type and Mutant PLS3 Localize to Mitochondria

We have produced a functional mutant of PLS3 with a mutagenesis approach analogous to that reported by Zhou *et al.* (32). The authors found that mutation of Phe[281] of the calcium-binding motif in PLS1 abolished function (32). We converted the corresponding Phe[258] in PLS3 to valine and generated stable transfectants of the mutant PLS3(F258V) in HEK293 cells. Transfectants of control (293-vector) and wild-type PLS3 (293-PLS3) were prepared similarly. Whole cell lysates of the G418-resistant clones were examined by Western blotting. Endogenous PLS3 could be detected in control whole cell lysates and transfectants expressing the wild-type or mutant PLS3 demonstrated increased levels of PLS3 (Fig. 1A). Subcellular fractionation indicated that the PLS3(F258V) protein localized to mitochondria, similar to the wild-type PLS3 (Fig. 1B). The integrity of cytosolic and mitochondrial fractions was confirmed by blotting for tubulin and voltage-dependent anion channel (VDAC), respectively (Fig. 1B). Similar transfectants were established in HeLa cells (not shown) for additional experiments described below.

Slow Growth in Cells Expressing PLS3(F258V) Mutant

The 293-vector, 293-PLS3, and 293-PLS3(F258V) cells were cultured over a 3-day period and serial cell counts were performed to monitor cell proliferation. The growth rate of 293-PLS3 cells was comparable to that of 293-vector cells, but 293-PLS3(F258V) cells grew at a slower rate (Fig. 1C), indicating that the PLS3(F258V) mutant interferes with cell growth. Cell cycle analysis revealed that the slow growth did not result from spontaneous G_1 or G_2-M arrest (not shown).

Expression of PLS3 Mutant Decreases Mitochondrial Mass and Transmembrane Potential

Because PLS3 localized to mitochondria and the growth of 293-PLS3(F258V) cells was slower than control cells, we suspected that mitochondria might be defective in cells expressing mutant PLS3. First, we analyzed the mitochondrial mass and membrane potential using JC-1 dye and flow cytometry. There were two peaks in JC-1 green fluorescence, corresponding to the mitochondrial mass (36). The low intensity peak was predominant in 293-vector cells and 293-PLS3(F258V) cells, while the higher intensity peak was more prominent in 293-PLS3 cells (Fig. 2A, *left*). Analysis of JC-1 red fluorescence, corresponding to the mitochondrial transmembrane potential (36), revealed a relative right shift in 293-
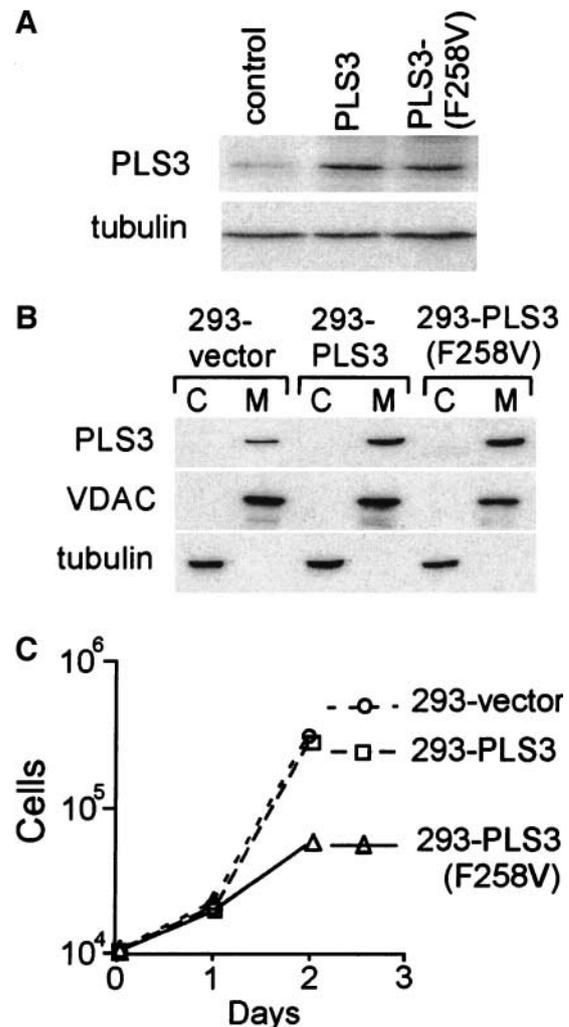

FIGURE 1. Stably transfected cell lines expressing wild-type PLS3 or mutant PLS3(F258V). **A.** G418-resistant clones of HEK293 cells transfected with pcDNA3.1 (*control*), pcDNA-PLS3, or pcDNA-PLS3(F258V) were harvested, and whole cell lysates analyzed by Western blotting with antibodies against PLS3 and tubulin. **B.** 293-vector, 293-PLS3, and 293-PLS3(F258V) cells were fractionated, and mitochondrial (*M*) and cytoplasmic (*C*) fractions were analyzed by Western blotting with antibodies against PLS3, VDAC, and tubulin. **C.** Growth curves of the 293-vector, 293-PLS3, and 293-PLS3(F258V) cells under normal growth conditions. Cells (10^4) were plated on day 0 and counted at days 1 and 2 by trypan blue exclusion.

PLS3 cells and left shift in 293-PLS3(F258V) cells (Fig. 2A, *right*). Similar results were obtained using Rhodamine 123 (Fig. 2B, *right*) with control 293-vector cells treated with 20 μM antimycin A, an inhibitor of mitochondrial electron transport complex, serving as an internal control (Fig. 2B, *left*). Thus, while overexpression of PLS3 was associated with increased mitochondrial mass and transmembrane potential, expression of PLS3(F258V) was associated with decreased mitochondrial mass and transmembrane potential.

Next, we quantitated in these cells several markers to correlate with changes of mitochondrial mass. As shown in Fig. 2C, levels of cytochrome *c* in whole cell lysates were dramatically reduced in 293-PLS3(F258V) cells compared to

293-vector and 293-PLS3 cells. By contrast, levels of VDAC were unaffected in 293-PLS3(F258V) cells and slightly increased in 293-PLS3 cells (Fig. 2C). Staining for cytosolic tubulin served as a loading control (Fig. 2C). Given the interaction of cytochrome c with mitochondrial CL, we determined the relative amounts of CL using the CL-specific fluorescence dye NAO (37, 38). As shown in Fig. 2D, CL levels were reduced in 293-PLS3(F258V) cells by almost 50% compared to control or 293-PLS3 cells. Finally, we quantified the amount of mitochondrial DNA by extracting DNA from purified mitochondria and did not detect any difference among 293-vector, 293-PLS3, and 293-PLS3(F258V) cells (not shown). Using a more sensitive real-time PCR technique with a set of mitochondrion-specific PCR primers as described (39), we found no difference in the copy number of mitochondrial encoded NADH dehydrogenase (subunit 1) in genomic DNAs from these three cell types (Fig. 2E).

Overexpression of PLS3 Mutant Reduces Intracellular ATP and Mitochondrial Respiration

The slower growth and reduced mitochondrial potential of 293-PLS3(F258V) cells suggested that mutant PLS3 interferes with mitochondrial respiration. We measured the total intracellular ATP levels by preparing trichloroacetic acid (TCA)-treated cell lysates for a luciferase assay (40). While the ATP concentration was 15% higher in 293-PLS3 cells compared to 293-vector cells, it was 10% lower ($P < 0.01$) in 293-PLS3(F258V) cells (Fig. 3A).

Next, we measured oxygen consumption in isolated mitochondria on incubation with succinate (substrate for state 4 respiration) and subsequently, after addition of ADP (for state 3 respiration). Compared to control and 293-PLS3 cells, the rate of oxygen consumption was reduced in 293-PLS3(F258V) cells (Fig. 3B). The rate of state 4 respiration was slightly lower in 293-PLS3(F258V) cells (3.5 ± 0.14 pmol/min/µg) compared to 293-vector (4.05 ± 0.21 pmol/min/µg) and 293-PLS3 cells (4.15 ± 0.21 pmol/min/µg; Fig. 3C). The rate of state 3 respiration in 293-PLS3 cells (17.5 ± 0.71 pmol/min/µg) was higher than control cells (15 ± 1.41 pmol/min/µg); whereas that of 293-PLS3(F258V) cells decreased by nearly 40% (9.85 ± 0.21 pmol/min/µg; Fig. 3C). The ratios of state 3 *versus* state 4 respiration (respiratory control ratio, RCR) are calculated as 3.70 (293-vector cells), 4.22 (293-PLS3 cells), and 2.81 (293-PLS3(F258V) cells). Thus, mitochondrial respiration was dramatically suppressed by expression of the PLS3(F258V) mutant and enhanced by overexpression of wild-type PLS3.

Gross Alterations in Mitochondrial Morphology in 293-PLS3(F258V) Cells

We next examined the mitochondria in these cells by electron microscopy. Mitochondria in 293-PLS3 cells were distinct from those in 293-vector cells, with fewer cristae present (Fig. 4, A and B). In contrast, 293-PLS3(F258V) cells
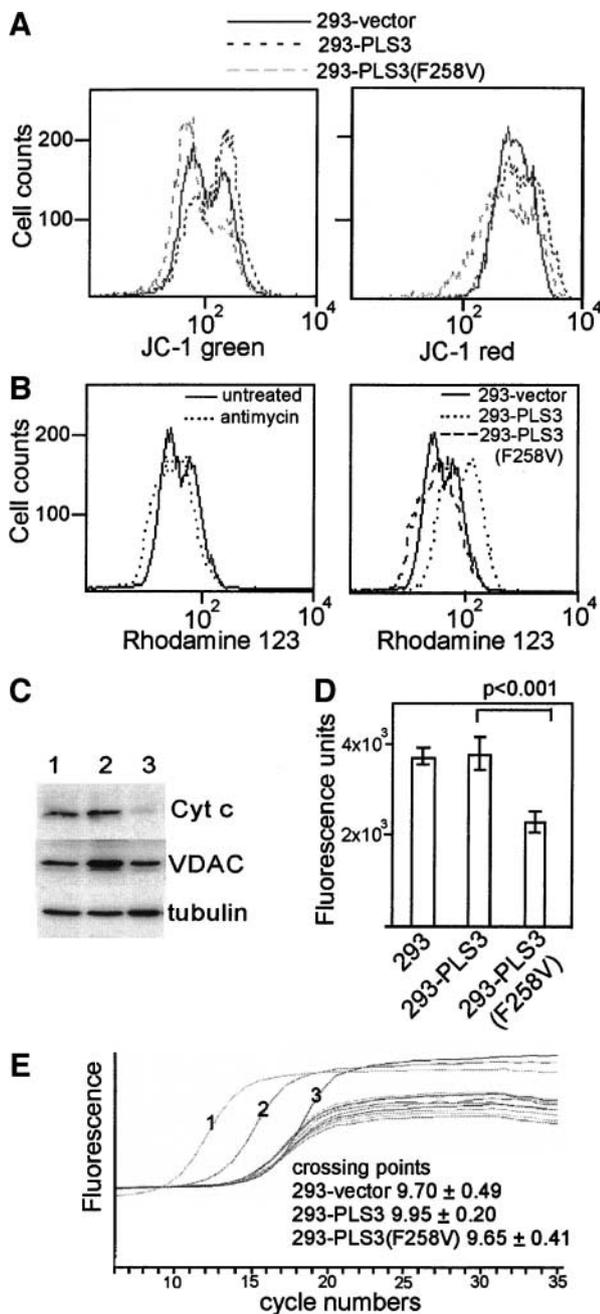

FIGURE 2. Overexpression of mutant PLS3 reduces mitochondrial mass, potential, and cytochrome c and CL content. **A.** 293-vector, 293-PLS3, and 293-PLS3(F258V) cells were incubated with JC-1 dye as indicated and green (*left panel*) and red (*right panel*) fluorescence were determined by flow cytometry. **B.** Flow cytometry curves for 293-vector, 293-PLS3, and 293-PLS3(F258V) cells stained with Rhodamine 123. The *left panel* shows the decrease of mitochondrial potential by treatment of 293-vector cells with 20 µM antimycin A for 6 h. The *right panel* shows the mitochondrial potential determined by Rhodamine 123. **C.** Western blotting of whole cell lysates from 293-vector (*lane 1*), 293-PLS3 (*lane 2*), and 293-PLS3(F258V) cells (*lane 3*). The blot was re-probed with antibodies to VDAC and tubulin for controls. **D.** 293-vector, 293-PLS3, and 293-PLS3(F258V) cells were stained with 10-N-nonyl-3,6-bis (dimethylamino) acridine orange (NAO), and fluorescence intensities at 570 nm were measured. *Error bars,* SDs from five independent measurements. **E.** Quantitative PCR analysis of mitochondrial NADH dehydrogenase in 400 ng of whole cell genomic DNA. *Curves 1–3,* different concentrations of standards; *other curves,* quantification of 293-vector, 293-PLS3, and 293-PLS3(F258V) in triplicates. The crossing points (in cycle numbers) of the three cells are indicated.
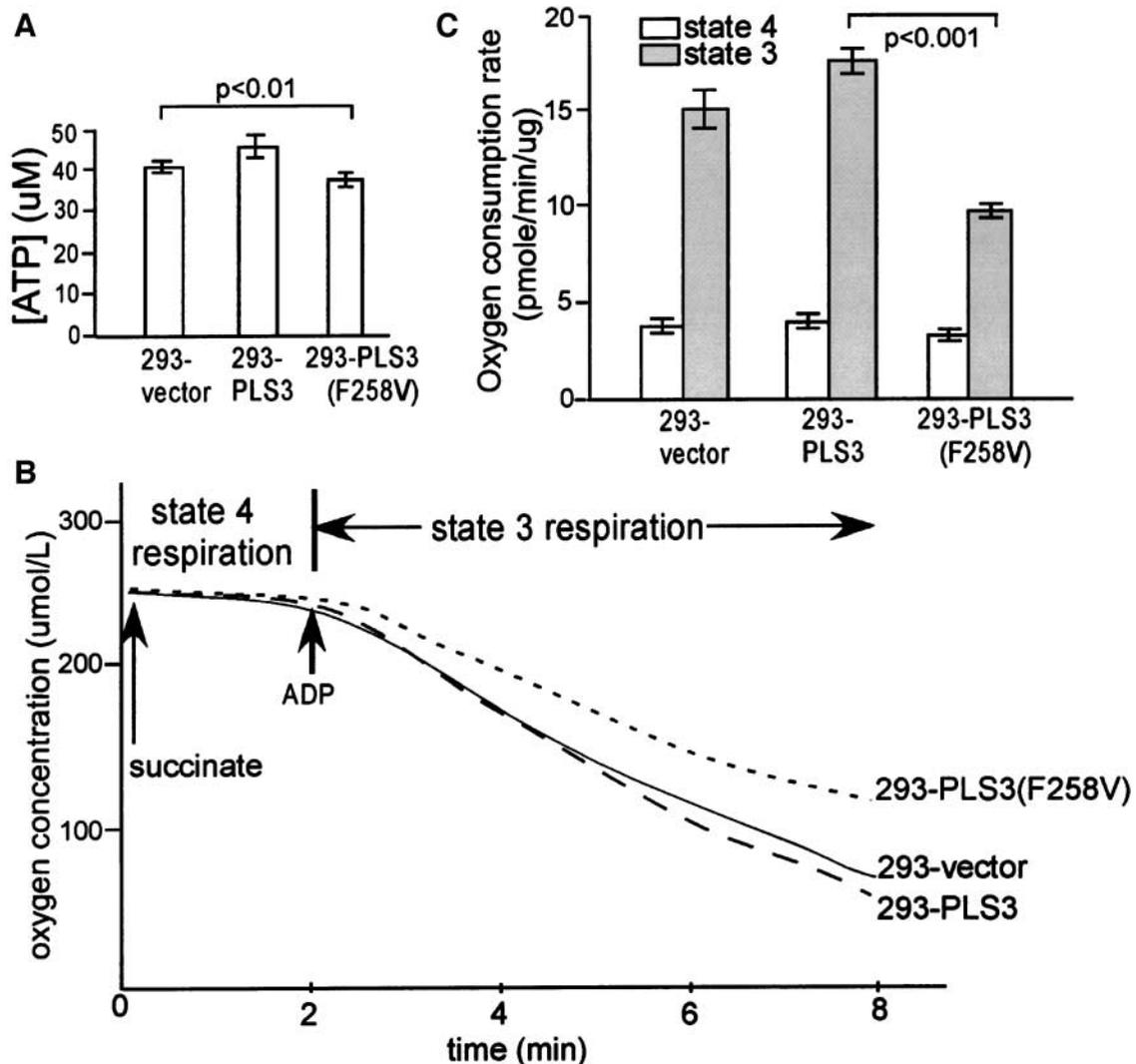
FIGURE 3. Overexpression of mutant PLS3 impairs mitochondrial respiration. **A.** Shown are ATP concentrations in 293-vector, 293-PLS3, and 293-PLS3(F258V) cells measured by luciferase assays. *Error bars,* means from five experiments. **B.** Mitochondria (50 μg) were isolated from 293-vector, 293-PLS3, and 293-PLS3(F258V) cells as indicated, placed in the Mitocell chamber, and oxygen concentrations were measured as described in the "Materials and Methods." **C.** Oxygen consumption rates (pmol/min/μg mitochondrial protein) were calculated from the slopes of each curve in **B**. *Error bars,* SDs from three independent experiments.

displayed few mitochondria, and these were notably large in size and abnormal in shape (Fig. 4C). They contained numerous cristae tightly packed together (Fig. 4C). Thus, perturbation of PLS3 by overexpression of wild-type or mutant PLS3 causes abnormal mitochondrial morphology.

Overexpression of PLS3 Changes the Susceptibility of UV-Induced Apoptosis

Given the central role of mitochondria in apoptosis (11), we sought to determine how overexpression of PLS3 might affect susceptibility to apoptosis. HeLa cell transfectants HeLa-vector, HeLa-PLS3, and HeLa-PLS3(F258V) were UV-irradiated and then assessed after 4 h for viability using 3-(4,5-dimethylth-iazol-2-yl)-2,5-diphenyltetrazolium bromide (MTT) assay. Cell viability after UV irradiation was 50% for HeLa-vector cells,

19.5% for HeLa-PLS3 cells, and 74% in HeLa-PLS3(F258V) cells (Fig. 5A). To confirm that the cell death was indeed apoptotic in nature, cells were also examined by Annexin V staining. As shown in Fig. 5B, UV irradiation increased the percentage of Annexin V-positive cells from 16% to 31% in HeLa-vector cells and from 20% to 38% in HeLa-PLS3 cells. By contrast, minimal change (11–15%) was detected in HeLa-PLS3(F258V) cells after UV irradiation (Fig. 5B). Thus, overexpression of PLS3 enhanced UV-induced apoptosis, while expression of mutant PLS3 was associated with resistance to apoptosis.

Next, we examined the effects of this UV treatment on mitochondrial mass and potential. As shown above (Fig. 2A), unirradiated 293-vector cells exhibited two populations based on JC-1 green fluorescence that reflect differences in mito-chondrial mass. Exposure to UV did not dramatically change

the distribution of these two populations (Fig. 5C). However, the JC-1 red analysis of the mitochondrial potential exhibited a shift of the curve to left after UV irradiation. In UV-treated 293-PLS3 cells, on the other hand, the JC-1 red curve shifted to the right (Fig. 5C). In 293-PLS3(F258V) cells, this pattern did not change after UV treatment (Fig. 5C), consistent with the resistance of these cells to UV-induced apoptosis.

UV Irradiation and PLS3 Overexpression Increase CL in Mitochondrial OM

To investigate a potential mechanistic role of PLS3 in apoptosis, we examined mitochondrial phospholipid changes in cells exposed to UV irradiation. Cellular phospholipids were labeled with $[^{32}P]P_i$, and phospholipids from mitochondrial membranes were analyzed by TLC. The efficacy of separation of mitochondrial IM and OM was assessed by the marker enzymes monoamine oxidase (MAO, an OM marker enzyme) and malate dehydrogenase (MDH, an IM/matrix marker enzyme; 41, 42). Both IM and OM fractions contained about 80% of the respective marker enzymes (Fig. 6A), similar to what has been reported in the literature (41). Comparing equal amounts of mitochondria from 293-vector cells before and after UV irradiation, we observed that levels of the most abundant phospholipid, phosphatidylcholine (PC), did not change after UV radiation; whereas CL and phosphatidylethanolamine (PE) levels increased after UV irradiation (Fig. 6, B and C). While the percentage of PE in the OM did not change with UV (Fig. 6B), the percentage of CL in the OM increased from 12% to 27% (Fig. 6, B and D). Similar studies were then performed in the same amounts of mitochondria from 293-PLS3 cells, the percentage of CL in the OM was elevated at 22% before UV treatment and further increased following UV radiation to 45% (Fig. 6C), suggesting that PLS3 facilitates CL transport from

IM to OM at steady state and during apoptosis. By contrast, in 293-PLS3(F258V) cells, there was baseline CL in the OM that did not increase after UV treatment (Fig. 6, C and D), suggesting that expression of PLS3 mutant prevents mitochondrial CL transport.

PLS3 Regulates tBid-Induced Mitochondrial Cytochrome c Release

Given that CL is the mitochondrial target of tBid (21), we hypothesized that PLS3-mediated CL transport to the mitochondrial OM may regulate susceptibility to tBid-induced apoptosis. Mitochondria isolated from HeLa-vector, HeLa-PLS3, and HeLa-PLS3(F258V) cells were incubated with recombinant tBid, and cytochrome c release was assessed by Western blotting of mitochondrial pellets and supernatants. Because the yield of mitochondria from HeLa-PLS3(F258V) cells was lower (Fig. 2), we balanced the total amount of mitochondria before the in vitro release study. While there was slightly greater cytochrome c release from mitochondria derived from HeLa-PLS3 cells than from HeLa-vector cells, there was less cytochrome c release from HeLa-PLS3(F258V) mitochondria (Fig. 7A). The amounts of cytochrome c and VDAC remaining in the mitochondrial pellets from the three cell types were roughly equivalent (Fig. 7A). Using densitometry, we calculated the percentages of cytochrome c release from HeLa-vector, HeLa-PLS3, and HeLa-PLS3(F258V) mitochondria to be 32.9%, 34.6%, and 18.9%, respectively (Fig. 7B). The effect of mitochondrial expression of PLS3 is not limited to cytochrome c release. We also tested the supernatants with SMAC antibody and found that SMAC release by recombinant tBid was greatly enhanced by overexpression of PLS3 and slightly suppressed by expression of PLS3(F258V) mutant (Fig. 7, A and B).
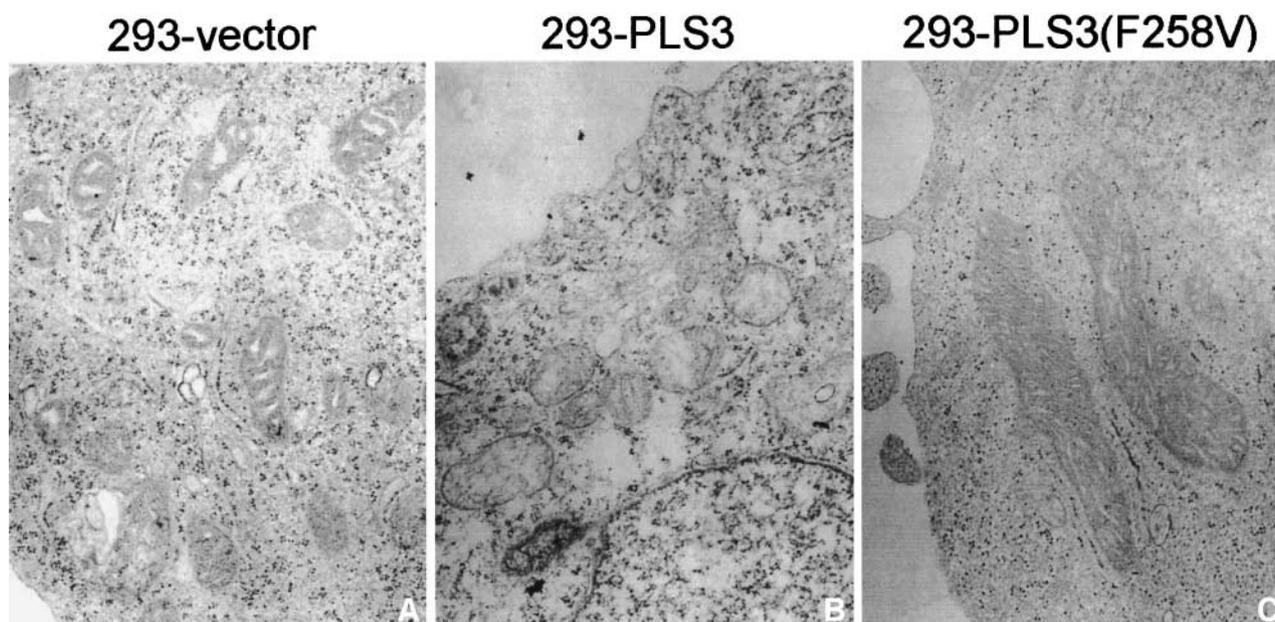

FIGURE 4. Aberrant mitochondrial structure in PLS3-targeted cells. Electron microscopic images of 293-vector (**A**), 293-PLS3 (**B**), and 293-PLS3 cells (**C**). All photographs are shown at 33,047 × magnification.
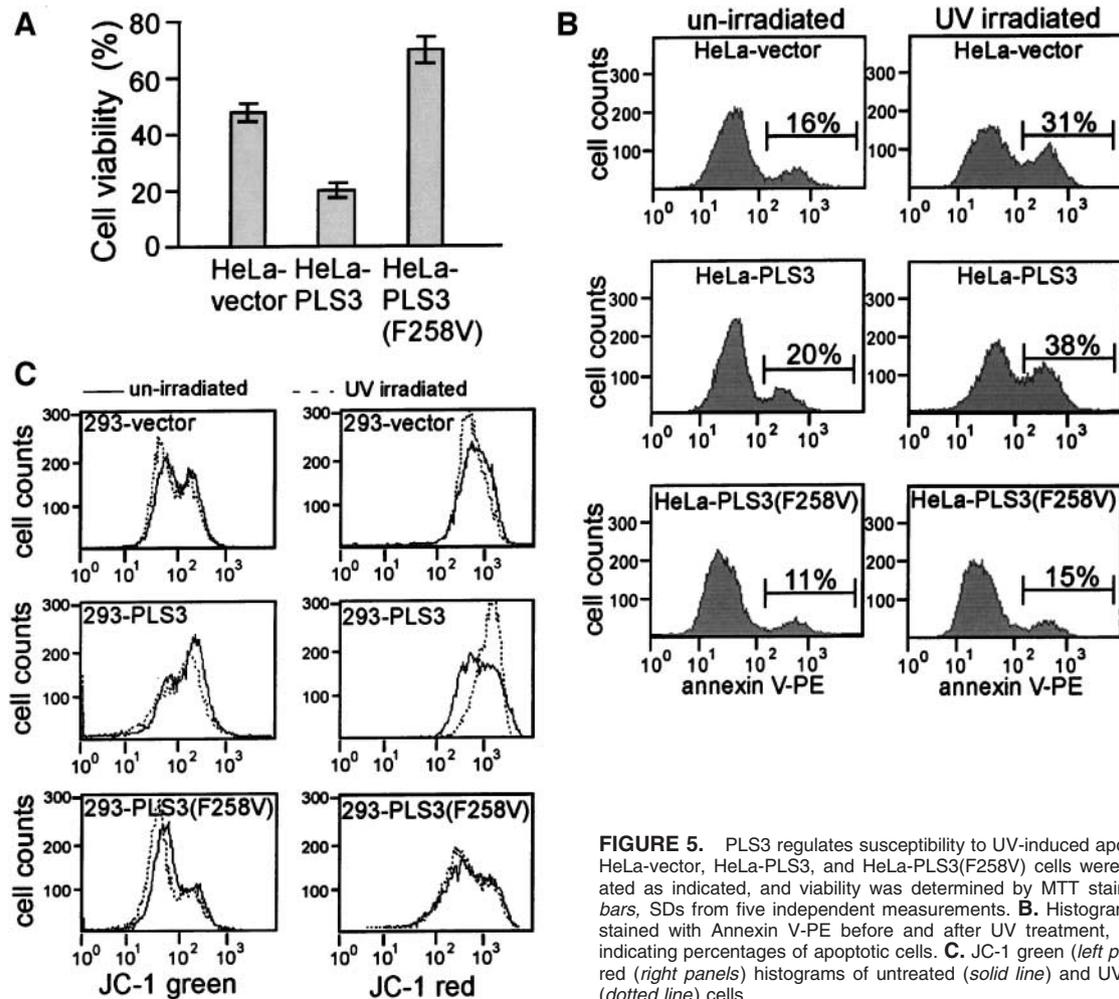
FIGURE 5. PLS3 regulates susceptibility to UV-induced apoptosis. **A.** HeLa-vector, HeLa-PLS3, and HeLa-PLS3(F258V) cells were UV-irradiated as indicated, and viability was determined by MTT staining. *Error bars,* SDs from five independent measurements. **B.** Histograms of cells stained with Annexin V-PE before and after UV treatment, with gates indicating percentages of apoptotic cells. **C.** JC-1 green (*left panels*) and red (*right panels*) histograms of untreated (*solid line*) and UV-irradiated (*dotted line*) cells.

Discussion

Phospholipid translocation events are important for multiple aspects of the apoptotic process. Translocation of PS from the inner to outer leaflet of the plasma membrane, for example, is critical for recognition and clearance of apoptotic cells by macrophages (9, 10). Here we demonstrate that translocation of CL from the mitochondrial IM to OM is regulated by the newly recognized PLS family member PLS3, which proves critical for maintaining normal mitochondrial apoptotic function. We found that disruption of CL transport to the mitochondrial OM, accomplished through overexpression of mutant PLS3, was not only associated with diminished apoptotic responsiveness but also with profound alterations in mitochondrial structure and oxidative function. Overexpression of PLS3, on the other hand, led to increased CL translocation to the mitochondrial OM that was associated with both enhanced respiration and apoptotic response.

The regulation of apoptotic responsiveness by PLS3 appears related to its role in mitochondrial CL transport. Garcia Fernandez *et al.* (43) have reported that intramitochondrial CL redistribution occurs as an early event in apoptosis. Due to the localization of CL synthase, mitochondrial CL is primarily (estimated 90%) present in the IM (44, 45). Thus, for normal apoptotic responses, CL must be transported to the OM for physical interaction with tBid (21) and for facilitating Bax-induced cytochrome c release (22), because both these proteins remain in the OM and would otherwise be inaccessible to CL in the IM. Using ^{32}P-labeling of phospholipids and biochemical fractionation of mitochondrial membranes to assess CL levels, we confirmed the predominant localization of CL to the IM and its translocation to OM during UV-induced apoptosis. The amounts of CL in the mitochondrial IM and OM before and after UV irradiation were also measured using capillary electrophoresis, and similar findings were obtained (46). Our finding that the OM fraction of CL increased in cells overexpressing PLS3 and decreased in cells expressing mutant PLS3 suggests a positive role for PLS3 in translocating CL to the OM. During UV-induced apoptosis, we observed enhanced CL translocation on overexpression of PLS3, while overexpression of mutant PLS3 suppressed translocation following UV treatment. The increased susceptibility to UV-induced apoptosis seen in cells overexpressing PLS3 is likely due to increased CL content in the OM that facilitates tBid recruitment and Bax activation. Our demonstration of increased cytochrome c and SMAC release induced by recombinant tBid from mitochondria isolated from HeLa-PLS3 compared to HeLa-vector cells is consistent with

this notion. Mitochondria from HeLa-PLS3(F258V) cells, by contrast, released far less cytochrome *c* in response to tBid compared to HeLa-vector cells (18.9% *versus* 32.9%). Thus, our studies demonstrate a clear relationship between CL transport to OM by intact PLS3 function and tBid-induced release of apoptogenic factors. Although we do not have evidence for translocation or synthesis of other mitochondrial phospholipids during apoptosis, based on the mitochondrial structural changes (47) and the finding that Bid itself has lipid transferase activity (48, 49), other mitochondrial lipid remodeling will be discovered in the future.

We found that disruption of PLS3 function resulted in profound morphological changes in the mitochondria. Mitochondria in 293-PLS3 cells have looser cristae than in 293-vector cells; whereas mitochondria in 293-PLS3(F258V) cells were sparse in number and of larger size, with densely packed cristae. This type of abnormal mitochondrial morphology

represents a novel phenotype. The morphology of mitochondria in 293-PLS3 cells is reminiscent to what was reported in CHO cells that are defective in biogenesis of phosphatidylglycerol and CL. In those studies (50, 51), mitochondria appeared greatly enlarged and swollen, and the cristae were disorganized. We observed similar morphology in the mitochondria of 293-PLS3 cells, but they have a normal level of CL. Overexpression of mutant PLS3 decreases the level of CL and creates a pattern of tightly packed cristae. This pattern suggests defects in the mitochondrial membranes that are consistent with decreased OM expansion and increased IM expansion. Given the IM localization of CL and the demonstrated role here of PLS3 in CL translocation, the abnormal cristae structure in 293-PLS3(F258V) cells probably results from retention and accumulation of phospholipids that PLS3 may transport in the mitochondrial IM and consequent failure of the OM to expand properly.
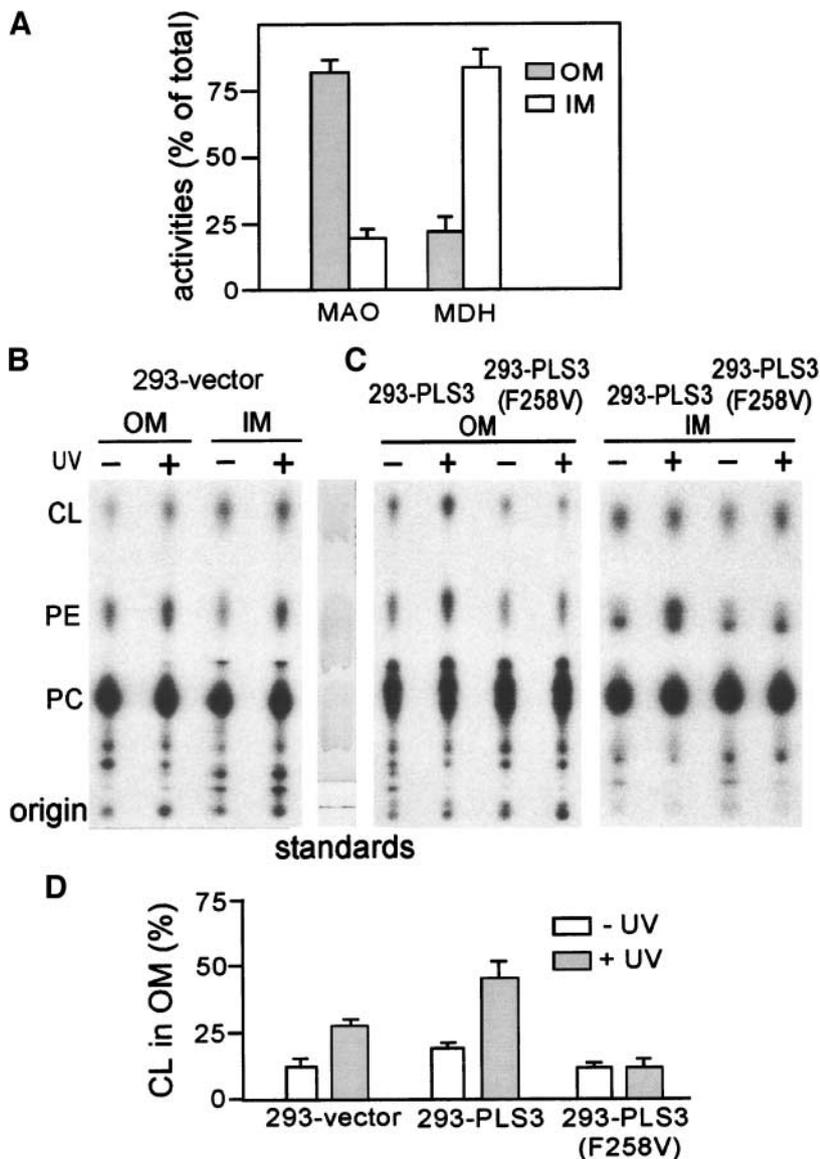

FIGURE 6. PLS3 regulates CL content and apoptotic translocation. **A.** Mitochondria were fractionated into IM and OM, and the percentages of enzyme activities of MAO and MDH in the mitochondrial OM and IM fractions were determined. **B.** 293-vector cells were labeled with [^{32}P]P$_i$, UV-treated, and then mitochondrial IM and OM were isolated and lipids extracted for TLC analysis. Migration of phosphatidylcholine (*PC*), phosphatidylethanolamine (*PE*), and CL was established by nonradioactive standards followed by iodine staining (*standards*). **C.** ^{32}P-labeled lipids were analyzed from equal amounts of mitochondria from 293-PLS3 or 293-PLS3(F258V) cells with or without UV irradiation as in **B**. **D.** Shown are percentages of CL present in the OM of unirradiated (*open bars*) and UV-treated (*shaded bars*) 293-vector, 293-PLS3, and 293-PLS3(F258V) cells, derived from the ratio of OM to the sum of OM and IM. *Error bars,* SDs from three experiments.
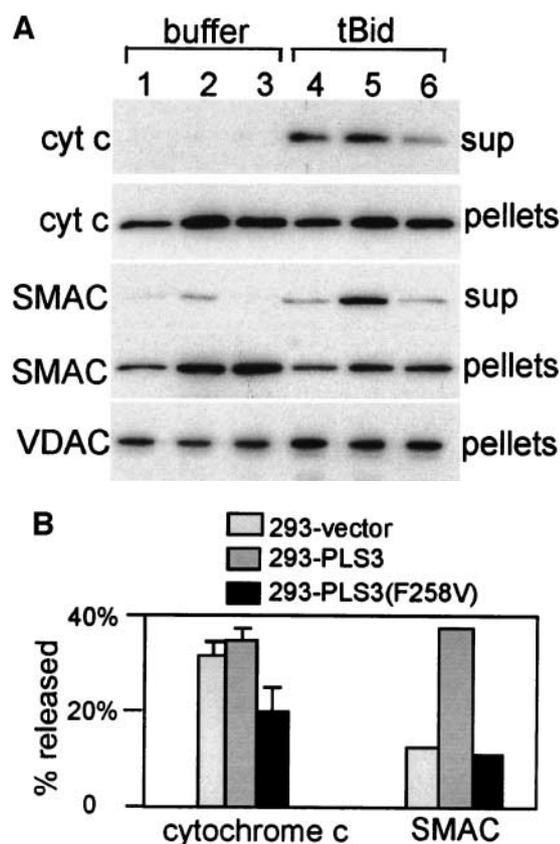
FIGURE 7. Effects of PLS3 on tBid-induced cytochrome *c* and SMAC release. **A.** Mitochondria (60 μg) isolated from HeLa-vector (*lanes 1* and *4*), HeLa-PLS3 (*lanes 2* and *5*), and HeLa-PLS3(F258V) cells (*lanes 3* and *6*) were incubated with buffer (*lanes 1–3*) or recombinant tBid (0.6 μg; *lanes 4–6*) for 20 min at 37°C. The supernatants and pellets were subjected to Western analysis for cytochrome *c*, SMAC, and VDAC. **B.** The bands of cytochrome *c* and SMAC in **A** were quantified by densitometry and the percentages of tBid-induced mitochondrial release are shown.

Two other studies have described apoptotic mitochondrial morphology. First, in a study by Frank *et al.* (52), mitochondria displayed a reticulo-tubular morphology and converted to a punctiform pattern during apoptosis. This process required translocation of Drp1 from the cytoplasm to mitochondrial division sites. Blocking Drp1 with a dominant negative mutant prevented the morphological conversion, release of cytochrome *c*, and cell death, implying that mitochondrial fission is an important step of apoptosis (52). In our study, the large size of mitochondria in 293-PLS3(F258V) cells suggests that their division may also be impaired. It would be interesting to test whether there is any defect in Drp1 targeting to the site of division in these cells. In the second study by Scorrano *et al.* (47), recombinant Bid was used to induce apoptosis in cell-free mitochondria so as to investigate cristae remodeling. Normal mitochondria displayed a partially condensed conformation with numerous narrow cristae that are connected to the OM by narrow tubular junctions. When mitochondria were incubated with recombinant tBid, cristae fused into larger compartments, and cristae junctions widened markedly (47). The mitochondrial morphology described here does not appear similar to

either of these studies. The relative resistance of mitochondria expressing PLS3(F258V) to tBid-induced cytochrome *c* release indicates that the membranous defects induced by blocking PLS3 may interfere with the remodeling of cristae during apoptosis.

It is unclear how changes in PLS3 activity interfere with CL synthesis. CL synthesis is initiated by conversion of CTP and phosphatidic acid to CDP-diacylglycerol and glycerol-3-phosphate by CTP:phosphatidic acid cytidylyltransferase. The products are metabolized by phosphatidylglycerophosphate (PGP) synthase to PGP. PGP loses one phosphate to become phosphatidylglycerol and is converted to CL by CL synthase (53, 54). Many factors can potentially regulate CL synthesis, including availability of ATP or plasma fatty acids in diabetes, ischemia and reperfusion, and hormonal regulation of PGP synthase (54, 55). Determination of the activities of enzymes involved in the CL synthesis may elucidate the mechanism of decreased CL in 293-PLS3(F258V) cells.

Examination of the mitochondria in our transfectants by JC-1 and Rhodamine staining suggested that PLS3, in addition to maintaining gross mitochondrial structure and apoptotic responsiveness, is also a determinant of mitochondrial mass and transmembrane potential. The abnormal mitochondrial structure in PLS3-targeted cells was correlated with decreased mitochondrial mass and potential, while overexpression of PLS3 was associated with increased mitochondrial mass and potential. Mitochondria in 293-PLS3 cells exhibited increased transmembrane potential after UV irradiation compared to loss of potential in UV-irradiated control cells. The JC-1 staining revealed two populations of cells: the population with greater mitochondrial mass appeared more metabolically active with respect to ATP production and oxidative phosphorylation, as reflected by higher ATP levels and state 3 respiration. This population increased in 293-PLS3 and decreased in PLS3(F258V) cells, suggesting that mitochondria in 293-PLS3(F258V) cells have defective oxidative respiration and poor oxygen consumption. This functional defect is likely related to their lower content of CL and cytochrome *c*, which was 50% of that in control and PLS3-transfected cells. Interestingly, levels of VDAC, which is unrelated to oxidative phosphorylation, were not affected by modulation of PLS3 in these cells. Mitochondrial DNA also remains unchanged. A previous connection between low CL and impaired respiration has been shown in a yeast mutant lacking CL synthase (56) or PGP synthase (53, 57).

In summary, our studies establish a central role for the PLS family member PLS3 in regulating mitochondrial structure and function. We conclude that the primary function of PLS3 is to mediate CL transport from the mitochondrial IM to OM, and disruption of this process ultimately leads to profound defects in mitochondrial architecture, mass and transmembrane potential, and apoptotic responsiveness.

Materials and Methods

Wild-Type PLS3 and PLS3(F258V) Transfectants

HEK293 cells and HeLa cells were maintained in DMEM supplemented with 10% FCS and penicillin/streptomycin. Mutation of Phe[258] in PLS3 to valine was carried out by

site-directed mutagenesis according to manufacturer's protocol (Clontech, Palo Alto, CA). The cDNAs encoding wild-type PLS3 and PLS3(F258V) were cloned into the expression vector pcDNA3.1 (Invitrogen, Carlsbad, CA), and transfected into HEK293 or HeLa cells using the calcium phosphate precipitation method. Transfected cells were selected with G418 (1 mg/ml) and resistant clones were picked and expanded for Western analysis using anti-PLS3 antibody. Polyclonal antibody was raised in rabbits against the NH$_2$-terminal 50 amino acids of PLS3 (Zymed Laboratories, San Francisco, CA) and purified by affinity chromatography before use (35). Monoclonal antibody against tubulin was from Santa Cruz Technology, Inc. (Santa Cruz, CA). Cytochrome *c* antibody was from BD Biosciences (San Diego, CA) and VDAC antibody was from Affinity BioReagents, Inc. (Golden, CO). SMAC antibody was from Imgenex (San Diego, CA).

Flow Cytometry Analysis

Flow cytometry was performed on a FACScan using Cell Quest software (Becton Dickinson, San Jose, CA) at the University of Utah core facility. To determine mitochondrial mass and transmembrane potential, cells were incubated with 10 μg/ml JC-1 or Rhodamine 123 (Molecular Probes, Eugene, OR) followed by flow cytometry (58). Cell cycle analysis was performed on ethanol-fixed cells stained with propidium iodide (50 μg/ml) before flow cytometry analysis.

Electron Microscopy

Cells were fixed overnight at 4°C in 0.1 M sodium cacodylate with 2.5% glutaraldehyde and 1% paraformaldehyde, with the addition of 2.4% sucrose and 8 mM CaCl$_2$, then washed twice with 0.1 M sodium cacodylate and refixed for 45 min in 2% osmium tetroxide in 0.1 M cacodylate buffer. After washing in water, cells were stained en bloc with saturated aqueous uranyl acetate for 1 h. After dehydration in a graded series of ethanol, infiltration was carried out through a series of ethanol:Spurr's plastic ratios and finally embedded in straight Spurr's plastic. Blocks were polymerized overnight in a 60°C oven and sectioned with a diamond knife to a thickness of 60–80 nm, and sections were picked up on 135 hex mesh grids. Sections were stained in saturated aqueous uranyl acetate followed by Reynold's lead citrate. All electron micrographs were taken on a Hitachi H-7100 transmission electron microscope at 75 kV.

Subcellular Fractionation and Preparation of Mitochondria and Mitoplasts

Mitochondria were isolated by differential centrifugation. Briefly, cells were washed once with mitochondria isolation buffer (MIB) containing 200 mM mannitol, 70 mM sucrose, 1 mM EGTA, and 10 mM HEPES (pH 7.4). After incubating for 10 min in ice-cold MIB containing 0.5 mg/ml BSA, cells were disrupted by passing through 25G needle 10 times. The homogenate was centrifuged at 800 × *g* for 5 min at 4°C. The supernatant was collected and spun at 10,000 × *g* for 10 min at 4°C, and the pellet was resuspended in MIB containing BSA as the crude mitochondria. The supernatant was centrifuged at 30,000 × *g* for 60 min to collect the cytoplasm.

To further fractionate mitochondria for isolation of OM and IM, crude mitochondria (400 μg by protein) were incubated in 2 ml KH$_2$PO$_4$ (10 mM) with stirring for 15 min at 4°C. Equal volume of a buffer containing 32% sucrose, 30% glycerol, 10 mM KH$_2$PO$_4$, and 10 mM MgCl$_2$ was added and stirred for another 15 min. Mitochondria were broken by passing through 25G needles 8 times followed by centrifugation at 12,000 × *g* for 10 min. The supernatant contains the OM, and the pellet contains mitoplasts. To determine the purity of separation, we measured the activities of MAO and MDH, as OM and IM markers as described (41).

Quantitation of Mitochondrial DNA

Whole cell genomic and mitochondrial DNAs were isolated by DNAzol (Molecular Research Center, Inc., Cincinnati, OH) according to the manufacturer's protocol, and dissolved in 8 mM NaOH before quantification. The copy number of mitochondrial DNA in whole cell genomic DNAs was determined by real-time PCR using a set of mitochondrion-specific PCR primers (5′ AACATACCCATGGCCAACCT and 5′ GGCAG-GAGTAATCAGAGGTG) that amplify NADH dehydrogenase (subunit 1) as described (39). Quantitative PCR was performed by the Roche LightCycler system (Roche Diagnostics GmbH, Mannheim, Germany) using SYBR Green I dye.

CL and Phospholipid Analysis

For CL quantitation, 10^6 cells were fixed with 4% formaldehyde in PBS for 10 min. CL was stained with 30 μM NAO (Molecular Probes; Refs. 37, 38), and the fluorescence intensities at 590 nm were measured using a Bio-Tek microplate reader. In pilot studies, we found that an NAO concentration of 15 μM was sufficient to saturate mitochondrial CL in 10^5 cells. For phospholipid analysis, cells were labeled with 0.5 mCi [^{32}P]P$_i$ per each 10-cm plate overnight before UV irradiation and harvesting. Cells were washed twice with cold PBS followed by mitochondria isolation and IM and OM fractionation. Phospholipids were extracted according to the standard method of Bligh and Dyer (59). Lipids were analyzed by TLC in a solvent system of chloroform-methanol-water-ammonium hydroxide 120:75:6:2 (v/v; 60) using Whatman silica TLC plates (Fisher Scientific, Pittsburgh, PA).

Cell Viability and Apoptosis

Cells were irradiated with unfiltered UV-B lamps (National Biological Corp., Twinsburg, OH) at 4 J/m^2/s over 2 min. Cell viability assays using MTT (Chemicon International Corp., Temecula, CA) were performed as described (61). Staining with Annexin V-PE (BD PharMingen, San Diego, CA) and flow cytometric analysis were performed according to the manufacturer's recommendations.

Intracellular ATP and Oxygen Consumption

For ATP quantitation, cells (1 × 10^7) were washed with cold PBS, lysed with 5% trichloroacetic acid, and the resulting supernatants were analyzed using a commercial ATP kit (Biotherma, Haninge, Sweden) and a MLX Microtiter plate Luminometer (Dynex Technologies, Inc, Chantilly, VA). State 3 and 4 mitochondrial oxygen consumption was measured at

25°C using a Mitocell connected to a two-channel dissolved oxygen measuring system (model #782, Strathkelvin Instrument, Glasgow, United Kingdom). Mitochondria were isolated from cells as described (62). Mitochondrial fractions (50 μg protein) were then diluted in respiration buffer [225 mM mannitol, 70 mM sucrose, 10 mM KH$_2$PO$_4$, and 1 mM EGTA (pH 7.2)]. For state 4 (steady state) respiration, succinate (Sigma Chemical Co., St. Louis, MO) was injected into the chamber at a final concentration of 7 mM and oxygen concentrations were monitored for 2 min. To measure state 3 (ADP-stimulated) respiration, ADP (Sigma) was then added at a final concentration of 150 μM for another 6 min.

Recombinant tBid-Induced Cytochrome c Release

The cDNA encoding tBid was cloned into pGEX6P-3 vector (Amersham-Pharmacia, Piscataway, NJ) and recombinant tBid was expressed in *Escherichia coli* as a fusion protein with glutathione *S*-transferase (GST). The fusion protein was purified with glutathione-Sepharose 4B affinity beads and cleaved by PreScission protease (Amersham-Pharmacia) in a buffer containing 50 mM Tris-HCl, 150 mM NaCl, 1 mM EDTA, and 1 mM DTT (pH 7.0). Mitochondria were incubated with the reaction buffer [250 mM sucrose, 20 mM HEPES, 10 mM KCl, 3 mM KH$_2$PO$_4$, 1.5 mM MgCl$_2$, 1 mM EGTA, 0.5 mg/ml BSA (pH 7.4)] with or without freshly made tBid at 25°C for 20 min, then the supernatants and pellets were separated by centrifugation (10,000 × *g*) for 10 min before Western analysis with antibodies against VDAC, cytochrome *c*, and SMAC. Bands were quantified by densitometry to calculate the percentage of release from mitochondria into supernatants.

Statistics

Data derived from multiple determinations were evaluated by *t* tests using Prism software (Graphpad, San Diego, CA). *P* values that are <0.05 were considered statistically significant.

Acknowledgments

References

1. Reed, J. C. Dysregulation of apoptosis in cancer. J. Clin. Oncol., *17:* 2941–2953, 1999.

2. Ionov, Y., Yamamoto, H., Krajewski, S., Reed, J. C., and Perucho, M. Mutational inactivation of the proapoptotic gene BAX confers selective advantage during tumor clonal evolution. Proc. Natl. Acad. Sci. USA, *97:* 10872–10877, 2000.

3. Green, D. R. and Evan, G. I. A matter of life and death. Cancer Cell, *1:* 19–30, 2002.

4. Cory, S. and Adams, J. M. Matters of life and death: programmed cell death at Cold Spring Harbor. Biochim. Biophys. Acta, *1377:* R25–R44, 1998.

5. Kroemer, G. and Reed, J. C. Mitochondrial control of cell death. Nat. Med., *6:* 513–519, 2000.

6. Fadok, V. A., Voelker, D. R., Campbell, P. A., Cohen, J. J., Bratton, D. L., and Henson, P. M. Exposure of phosphatidylserine on the surface of apoptotic lymphocytes triggers specific recognition and removal by macrophages. J. Immunol., *148:* 2207–2216, 1992.

7. Bratton, D. L., Fadok, V. A., Richter, D. A., Kailey, J. M., Guthrie, L. A., and Henson, P. M. Appearance of phosphatidylserine on apoptotic cells requires calcium-mediated nonspecific flip-flop and is enhanced by loss of the aminophospholipid translocase. J. Biol. Chem., *272:* 26159–26165, 1997.

8. Martin, S. J., Reutelingsperger, C. P., McGahon, A. J., Rader, J. A., van Schie, R. C., LaFace, D. M., and Green, D. R. Early redistribution of plasma membrane phosphatidylserine is a general feature of apoptosis regardless of the initiating stimulus: inhibition by overexpression of Bcl-2 and Abl. J. Exp. Med., *182:* 1545–1556, 1995.

9. Fadok, V. A., de Cathelineau, A., Daleke, D. L., Henson, P. M., and Bratton, D. L. Loss of phospholipid asymmetry and surface exposure of phosphatidylserine is required for phagocytosis of apoptotic cells by macrophages and fibroblasts. J. Biol. Chem., *276:* 1071–1077, 2001.

10. Fadok, V. A., Bratton, D. L., Rose, D. M., Pearson, A., Ezekewitz, R. A., and Henson, P. M. A receptor for phosphatidylserine-specific clearance of apoptotic cells [see comments]. Nature, *405:* 85–90, 2000.

11. Brenner, C. and Kroemer, G. Apoptosis. Mitochondria—the death signal integrators. Science, *289:* 1150–1151, 2000.

12. Parrish, J., Li, L., Klotz, K., Ledwich, D., Wang, X., and Xue, D. Mitochondrial endonuclease G is important for apoptosis in *C. elegans*. Nature, *412:* 90–94, 2001.

13. Li, L. Y., Luo, X., and Wang, X. Endonuclease G is an apoptotic DNase when released from mitochondria. Nature, *412:* 95–99, 2001.

14. Du, C., Fang, M., Li, Y., Li, L., and Wang, X. Smac, a mitochondrial protein that promotes cytochrome *c*-dependent caspase activation by eliminating IAP inhibition [In Process Citation]. Cell, *102:* 33–42, 2000.

15. Verhagen, A. M., Ekert, P. G., Pakusch, M., Silke, J., Connolly, L. M., Reid, G. E., Moritz, R. L., Simpson, R. J., and Vaux, D. L. Identification of DIABLO, a mammalian protein that promotes apoptosis by binding to and antagonizing IAP proteins [In Process Citation]. Cell, *102:* 43–53, 2000.

16. Susin, S. A., Lorenzo, H. K., Zamzami, N., Marzo, I., Snow, B. E., Brothers, G. M., Mangion, J., Jacotot, E., Costantini, P., Loeffler, M., Larochette, N., Goodlett, D. R., Aebersold, R., Siderovski, D. P., Penninger, J. M., and Kroemer, G. Molecular characterization of mitochondrial apoptosis-inducing factor. Nature, *397:* 441–446, 1999.

17. Li, H., Kolluri, S. K., Gu, J., Dawson, M. I., Cao, X., Hobbs, P. D., Lin, B., Chen, G., Lu, J., Lin, F., Xie, Z., Fontana, J. A., Reed, J. C., and Zhang, X. Cytochrome *c* release and apoptosis induced by mitochondrial targeting of nuclear orphan receptor TR3. Science, *289:* 1159–1164, 2000.

18. Karuman, P., Gozani, O., Odze, R. D., Zhou, X. C., Zhu, H., Shaw, R., Brien, T. P., Bozzuto, C. D., Ooi, D., Cantley, L. C., and Yuan, J. The Peutz-Jegher gene product LKB1 is a mediator of p53-dependent cell death. Mol. Cell, *7:* 1307–1319, 2001.

19. Luo, X., Budihardjo, I., Zou, H., Slaughter, C., and Wang, X. Bid, a Bcl2 interacting protein, mediates cytochrome *c* release from mitochondria in response to activation of cell surface death receptors. Cell, *94:* 481–490, 1998.

20. Zha, J., Weiler, S., Oh, K. J., Wei, M. C., and Korsmeyer, S. J. Posttranslational N-myristoylation of BID as a molecular switch for targeting mitochondria and apoptosis. Science, *290:* 1761–1765, 2000.

21. Lutter, M., Fang, M., Luo, X., Nishijima, M., Xie, X., and Wang, X. Cardiolipin provides specificity for targeting of tBid to mitochondria. Nat. Cell Biol., *2:* 754–761, 2000.

22. Kuwana, T., Mackey, M. R., Perkins, G., Ellisman, M. H., Latterich, M., Schneiter, R., Green, D. R., and Newmeyer, D. D. Bid, bax, and lipids cooperate to form supramolecular openings in the outer mitochondrial membrane. Cell, *111:* 331–342, 2002.

23. Wei, M. C., Lindsten, T., Mootha, V. K., Weiler, S., Gross, A., Ashiya, M., Thompson, C. B., and Korsmeyer, S. J. tBID, a membrane-targeted death ligand, oligomerizes BAK to release cytochrome *c*. Genes Dev., *14:* 2060–2071, 2000.

24. Wei, M. C., Zong, W. X., Cheng, E. H., Lindsten, T., Panoutsakopoulou, V., Ross, A. J., Roth, K. A., MacGregor, G. R., Thompson, C. B., and Korsmeyer, S. J. Proapoptotic BAX and BAK: a requisite gateway to mitochondrial dysfunction and death. Science, *292:* 727–730, 2001.

25. Korsmeyer, S. J., Wei, M. C., Saito, M., Weiler, S., Oh, K. J., and Schlesinger, P. H. Pro-apoptotic cascade activates BID, which oligomerizes BAK or BAX into pores that result in the release of cytochrome *c*. Cell Death Differ., *7:* 1166–1173, 2000.

26. Bevers, E. M., Comfurius, P., Dekkers, D. W., and Zwaal, R. F. Lipid translocation across the plasma membrane of mammalian cells. Biochim. Biophys. Acta, *1439:* 317–330, 1999.

27. Wiedmer, T., Zhou, Q., Kwoh, D. Y., and Sims, P. J. Identification of three new members of the phospholipid scramblase gene family. Biochim. Biophys. Acta, *1467:* 244–253, 2000.

28. Zhou, Q., Zhao, J., Stout, J. G., Luhm, R. A., Wiedmer, T., and Sims, P. J. Molecular cloning of human plasma membrane phospholipid scramblase. A protein mediating transbilayer movement of plasma membrane phospholipids. J. Biol. Chem., *272:* 18240–18244, 1997.

29. Zhou, Q., Zhao, J., Wiedmer, T., and Sims, P. J. Normal hemostasis but defective hematopoietic response to growth factors in mice deficient in phospholipid scramblase 1. Blood, 99: 4030–4038, 2002.

30. Zhao, J., Zhou, Q., Wiedmer, T., and Sims, P. J. Level of expression of phospholipid scramblase regulates induced movement of phosphatidylserine to the cell surface. J. Biol. Chem., 273: 6603–6606, 1998.

31. Williamson, P., Christie, A., Kohlin, T., Schlegel, R. A., Comfurius, P., Harmsma, M., Zwaal, R. F., and Bevers, E. M. Phospholipid scramblase activation pathways in lymphocytes. Biochemistry, 40: 8065–8072, 2001.

32. Zhou, Q., Sims, P. J., and Wiedmer, T. Identity of a conserved motif in phospholipid scramblase that is required for Ca^{2+}-accelerated transbilayer movement of membrane phospholipids. Biochemistry, 37: 2356–2360, 1998.

33. Frasch, S. C., Henson, P. M., Kailey, J. M., Richter, D. A., Janes, M. S., Fadok, V. A., and Bratton, D. L. Regulation of phospholipid scramblase activity during apoptosis and cell activation by protein kinase Cδ. J. Biol. Chem., 275: 23065–23073, 2000.

34. Sun, J., Zhao, J., Schwartz, M. A., Wang, J. Y., Wiedmer, T., and Sims, P. J. c-Abl tyrosine kinase binds and phosphorylates phospholipid scramblase 1. J. Biol. Chem., 276: 28984–28990, 2001.

35. Liu, J., Chen, J., Dai, Q., and Lee, R. M. Phospholipid scramblase 3 is the mitochondrial target of protein kinase C δ-induced apoptosis. Cancer Res., 63: 1153–1156, 2003.

36. Camilleri-Broet, S., Vanderwerff, H., Caldwell, E., and Hockenbery, D. Distinct alterations in mitochondrial mass and function characterize different models of apoptosis. Exp. Cell Res., 239: 277–292, 1998.

37. Erbrich, U., Septinus, M., Naujok, A., and Zimmermann, H. W. Hydrophobic acridine dyes for fluorescence staining of mitochondria in living cells. 2. Comparison of staining of living and fixed HeLa-cells with NAO and DPPAO. Histochemistry, 80: 385–388, 1984.

38. Septinus, M., Berthold, T., Naujok, A., and Zimmermann, H. W. Hydrophobic acridine dyes for fluorescent staining of mitochondria in living cells. 3. Specific accumulation of the fluorescent dye NAO on the mitochondrial membranes in HeLa cells by hydrophobic interaction. Depression of respiratory activity, changes in the ultrastructure of mitochondria due to NAO. Increase of fluorescence in vital stained mitochondria in situ by irradiation. Histochemistry, 82: 51–66, 1985.

39. Hail, N., Jr., Youssef, E. M., and Lotan, R. Evidence supporting a role for mitochondrial respiration in apoptosis induction by the synthetic retinoid CD437. Cancer Res., 61: 6698–6702, 2001.

40. Lundin, A. Use of firefly luciferase in ATP-related assays of biomass, enzymes, and metabolites. Methods Enzymol., 305: 346–370, 2000.

41. Ragan, C. I., Wilson, M. T., Darley-Usmar, V. M., and Lowe, P. N. Sub-fractionation of mitochondria and isolation of the proteins of oxidative phosphorylation. In: V. M. Darley-Usmar (ed.), Mitochondria, A Practical Approach, pp. 79–111. Oxford, England: IRL Press, 1987.

42. Daum, G., Bohni, P. C., and Schatz, G. Import of proteins into mitochondria. Cytochrome b2 and cytochrome c peroxidase are located in the intermembrane space of yeast mitochondria. J. Biol. Chem., 257: 13028–13033, 1982.

43. Garcia Fernandez, M., Troiano, L., Moretti, L., Nasi, M., Pinti, M., Salvioli, S., Dobrucki, J., and Cossarizza, A. Early changes in intramitochondrial cardiolipin distribution during apoptosis. Cell Growth & Differ., 13: 449–455, 2002.

44. Hoch, F. L. Cardiolipins and biomembrane function. Biochim. Biophys. Acta, 1113: 71–133, 1992.

45. Schlame, M., Rua, D., and Greenberg, M. L. The biosynthesis and functional role of cardiolipin. Prog. Lipid Res., 39: 257–288, 2000.

46. Qi, L., Danielson, N. D., Dai, Q., and Lee, R. M. Capillary electrophoresis of cardiolipin with on-line dye interaction and spectrophotometric detection. Electrophoresis, 24: 1680–1686, 2003.

47. Scorrano, L., Ashiya, M., Buttle, K., Weiler, S., Oakes, S. A., Mannella, C. A., and Korsmeyer, S. J. A Distinct pathway remodels mitochondrial cristae and mobilizes cytochrome c during apoptosis. Dev. Cell, 2: 55–67, 2002.

48. Esposti, M. D., Erler, J. T., Hickman, J. A., and Dive, C. Bid, a widely expressed proapoptotic protein of the Bcl-2 family, displays lipid transfer activity. Mol. Cell. Biol., 21: 7268–7276, 2001.

49. Esposti, M. D. Lipids, cardiolipin and apoptosis: a greasy licence to kill. Cell Death Differ., 9: 234–236, 2002.

50. Ohtsuka, T., Nishijima, M., Suzuki, K., and Akamatsu, Y. Mitochondrial dysfunction of a cultured Chinese hamster ovary cell mutant deficient in cardiolipin. J. Biol. Chem., 268: 22914–22919, 1993.

51. Kawasaki, K., Kuge, O., Chang, S. C., Heacock, P. N., Rho, M., Suzuki, K., Nishijima, M., and Dowhan, W. Isolation of a Chinese hamster ovary (CHO) cDNA encoding phosphatidylglycerophosphate (PGP) synthase, expression of which corrects the mitochondrial abnormalities of a PGP synthase-defective mutant of CHO-K1 cells. J. Biol. Chem., 274: 1828–1834, 1999.

52. Frank, S., Gaume, B., Bergmann-Leitner, E. S., Leitner, W. W., Robert, E. G., Catez, F., Smith, C. L., and Youle, R. J. The role of dynamin-related protein 1, a mediator of mitochondrial fission, in apoptosis. Dev. Cell, 1: 515–525, 2001.

53. McMillin, J. B. and Dowhan, W. Cardiolipin and apoptosis. Biochim. Biophys. Acta, 1585: 97–107, 2002.

54. Hatch, G. M. Cardiolipin: biosynthesis, remodeling and trafficking in the heart and mammalian cells (Review). Int. J. Mol. Med., 1: 33–41, 1998.

55. Hatch, G. M. Regulation of cardiolipin biosynthesis in the heart. Mol. Cell. Biochem., 159: 139–148, 1996.

56. Koshkin, V. and Greenberg, M. L. Oxidative phosphorylation in cardiolipin-lacking yeast mitochondria. Biochem. J., 347 (Pt. 3): 687–691, 2000.

57. Ostrander, D. B., Zhang, M., Mileykovskaya, E., Rho, M., and Dowhan, W. Lack of mitochondrial anionic phospholipids causes an inhibition of translation of protein components of the electron transport chain. A yeast genetic model system for the study of anionic phospholipid function in mitochondria. J. Biol. Chem., 276: 25262–25272, 2001.

58. Esposti, M. Assessing functional integrity of mitochondria in vitro and in vivo. Methods Cell Biol., 65: 75–96, 2001.

59. Bligh, E. A. and Dyer, W. J. Method for lipid extraction. Can. J. Biochem. Physiol., 37: 911–917, 1959.

60. Fine, J. B. and Sprecher, H. Unidimensional thin-layer chromatography of phospholipids on boric acid-impregnated plates. J. Lipid Res., 23: 660–663, 1982.

61. Mosmann, T. Rapid colorimetric assay for cellular growth and survival: application to proliferation and cytotoxicity assays. J. Immunol. Methods, 65: 55–63, 1983.

62. Gottlieb, E., Armour, S. M., and Thompson, C. B. Mitochondrial respiratory control is lost during growth factor deprivation. Proc. Natl. Acad. Sci. USA, 99: 12801–12806, 2002.

Phospholipid Scramblase 3 Controls Mitochondrial Structure, Function, and Apoptotic Response [1]1NIH grants K08CA795093 (R.M.L.) and K08AR48618 (D.G.); Huntsman Cancer Foundation.

Jihua Liu, Qiang Dai, Jun Chen, et al.

Updated version	Access the most recent version of this article at: http://mcr.aacrjournals.org/content/1/12/892

Cited articles	This article cites 59 articles, 26 of which you can access for free at: http://mcr.aacrjournals.org/content/1/12/892.full#ref-list-1
Citing articles	This article has been cited by 21 HighWire-hosted articles. Access the articles at: http://mcr.aacrjournals.org/content/1/12/892.full#related-urls

E-mail alerts	Sign up to receive free email-alerts related to this article or journal.
Reprints and Subscriptions	To order reprints of this article or to subscribe to the journal, contact the AACR Publications Department at pubs@aacr.org.
Permissions	To request permission to re-use all or part of this article, use this link http://mcr.aacrjournals.org/content/1/12/892. Click on "Request Permissions" which will take you to the Copyright Clearance Center's (CCC) Rightslink site.